Biosynthesis-Guided Discovery of Enteropeptins, Unusual Sactipeptides Containing an *N*-Methylornithine

Kenzie A. Clark,[1] Brett C. Covington,[1] and Mohammad R. Seyedsayamdost[1,2,*]

[1]Department of Chemistry, Princeton University, Princeton, NJ 08544

[2]Department of Molecular Biology, Princeton University, Princeton, NJ 08544

*Correspondence should be addressed to M.R.S.: mrseyed@princeton.edu

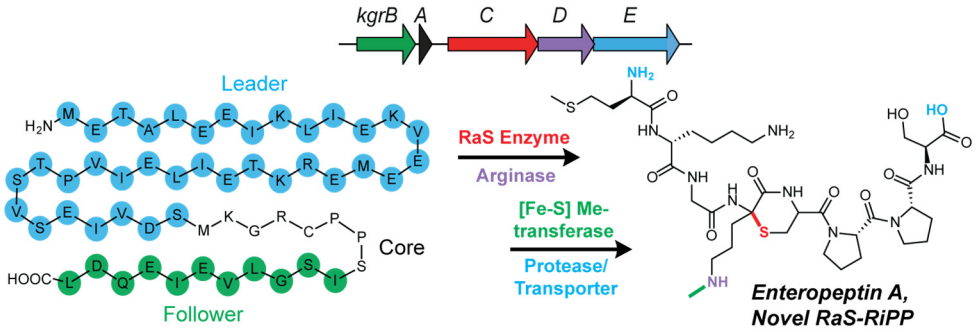

Abstract

The combination of next-generation DNA sequencing technologies and bioinformatics have revitalized natural product discovery. Using a new bioinformatic search strategy, we recently identified ~600 gene clusters in animal microbiomes that code for ribosomal peptide natural products synthesized by radical S-adenosylmethionine enzymes. These grouped into 16 subfamilies and pointed to an unexplored microbiome biosynthetic landscape. Herein, we report the structure, biosynthesis, and function of one of these natural product groups, that we term enteropeptins, from the gut microbe *Enterococcus cecorum*. We elucidate three novel reactions, each catalyzed by a different family of metalloenzymes, in the biosynthesis of enteropeptins. Among these, we characterize the founding member of a widespread superfamily of Fe-S-containing methyltransferases, which, together with a di-Mn-dependent arginase, installs an *N*-methylornithine in the peptide sequence. Biological assays with the mature product revealed bacteriostatic activity only against the producing strain, extending an emerging theme of fratricidal or self-inhibitory metabolites in microbiome firmicutes.

Introduction

Natural products have provided a rich source of complex enzymatic chemistries, therapeutic lead compounds, and new paradigms in biology. Some of the most well-known natural products, such as vancomycin and penicillin, are synthesized by large assembly line non-ribosomal peptide synthetase (NRPS) complexes.[1] An alternative strategy is provided by ribosomally-synthesized and post-translationally modified peptides (RiPPs), in which the ribosome synthesizes a short genetically encoded peptide that is then transformed into the final mature product by, usually, a small number of tailoring enzymes.[2] This strategy is particularly wide-spread in organisms with petit, host-adapted genomes such as the firmicutes, as RiPP biosynthetic gene clusters (BGCs) have small genomic footprints. Aside from hosting numerous unexplored RiPP BGCs, the firmicutes are also important due to their abundance in diverse animal microbiomes where the molecules they secrete have the potential to influence host health.[3-5]

Because of their small size and lack of unifying genetic features, RiPP BGCs initially proved difficult to identify with standard approaches, and new methods have recently emerged for this purpose.[2,6-9] We have contributed to the cadre of available approaches with a biosynthesis-regulation co-occurrence strategy.[5] Using the streptide biosynthetic operon as a reference,[10,11] we searched for RiPP gene clusters that are built by one or more radical S-adenosylmethionine (RaS) enzymes and regulated by quorum sensing (QS), reasoning that the resulting natural products would be novel, owing to the remarkable versatility of the RaS enzyme superfamily,[12,13] and physiologically relevant, as QS has been shown to regulate important microbial behaviors, such as virulence and biofilm formation.[14,15] This search revealed ~600 RiPP BGCs, which grouped into 16 subfamilies based on precursor peptide sequence similarity, in mammalian microbiome streptococci alone (Fig. 1a).[10] Our subsequent mining of this network has revealed novel RaS enzyme chemistry and natural products, such as tetrahydro[5,6]benzindole formation in the tryglysins,[10,16] atypical sactionine topology in streptosactin and the *QMP* operon,[17,18] the first α-ether and β-thioether linkages by the *TQQ* and *NxxC* operons, respectively,[19,20] and a novel arginine-tyrosine crosslink by a RaS enzyme in the *RRR* cluster.[21] Interestingly, mature products from these clusters have revealed compelling bioactivities, with tryglysins proving to be nanomolar inhibitors of the pathogen *Streptococcus pneumoniae*,[16] and streptosactin exhibiting the first small molecule fratricidal activity with nanomolar potency.[17]

The gene clusters examined thus far contained simple architectures, consisting of a single RaS enzyme, with or without a discrete RiPP recognition element,[22] and a precursor peptide. Herein, we turn our attention to the most complex subfamily in our network, which contains a RaS enzyme, a hypothetical iron-sulfur cluster protein, and a predicted Mn-dependent arginase homolog. Using *in vitro* biochemistry, we elucidate the reaction carried out by each of these metalloenzymes and find that the RaS enzyme installs an α-thioether bond joining neighboring Cys and Arg residues to form an unusual six-membered thiomorpholine heterocycle, an alternative to the macrocyclic topology of previously identified sactipeptides. The modified arginine residue is then deguanidinated to ornithine by the arginase and *N*-methylated by the Fe-S protein with the use of SAM, resulting in the first reported instance of *N*-methylornithine in a RiPP. The Fe-S-dependent methyltransferase is the first characterized member of a new, prevalent superfamily of enzymes. Knowledge regarding the biosynthetic reactions allowed us to identify the mature natural products, which we name enteropeptin A-C, from the gut bacterium *Enterococcus cecorum.* Biological activity assays with enteropeptin A show species-specific bacteriostatic activity only against the producing strain, extending an emerging theme of self-inhibitory RiPPs produced by firmicutes, notably those in animal microbiomes.

Results & Discussion

The KGR Subfamily. The *KGR* subfamily from our original network, named for the conserved *C*-terminal KGR motif, contains 23 unique clusters from *S. thermophilus.* It encodes a 49mer precursor peptide (KgrA), a putative Fe-S cluster protein (KgrB), which does not belong to the RaS superfamily and exhibits no discernible homology to known enzymes, a RaS enzyme (KgrC), a protein with sequence similarity to arginase (KgrD), which uses a di-manganese cofactor to convert free arginine to ornithine in the urea cycle,[23,24] and finally a combination protease/exporter (KgrE) (Fig. 1b). We sought to elucidate the reactions of these enzymes with an *in vitro* approach in which the enzymes and precursor peptide would be generated recombinantly and reaction products elucidated with high-resolution mass spectrometry (HR-MS), tandem HR-MS (HR-MS/MS), and multi-dimensional NMR spectroscopy.

After repeated attempts to obtain soluble RaS enzyme (KgrC) from *S. thermophilus* failed, we performed additional bioinformatic searches and identified a highly homologous *kgr* cluster from several *Enterococcus cecorum* strains (Supplementary Table 1). *E. cecorum* is a commensal

strain isolated from chicken digestive tracts and has increasingly acted as an opportunistic human pathogen, causing outbreaks of enterococcal spondylitis in commercial poultry production.[25] We focused on the *kgr* cluster from *E. cecorum* ATCC 43198, which encodes the same set of modification enzymes as its *S. thermophilus* counterpart with a 56mer precursor peptide (Fig. 1b). The cluster is regulated by an upstream divergently transcribed LytTR-type transcriptional regulator.[26] A logo plot of the precursor peptide, generated from both the *Enterococcus* and *Streptococcus* clusters, shows that the KGRCPP motif is conserved (Fig. 1c).

Characterization of the KGR Biosynthetic Enzymes. To determine the nature of the modifications installed by KgrBCD onto KgrA, we produced each protein individually as a hexaHis-tagged construct via recombinant expression in *E. coli* (Supplementary Tables 2-3). As KgrB and KgrC were predicted to contain [Fe-S] clusters, they were purified anaerobically. The UV-vis absorption spectra of these proteins were similar and contained a broad peak at 410 nm consistent with the presence of at least one $[4Fe\text{-}4S]^{2+}$ cluster (Supplementary Fig. 1). Quantification of Fe and labile sulfide revealed 2.9 ± 0.1 Fe and 3.5 ± 0.1 S^{2-} per KgrB protomer, while KgrC contained 3.9 ± 0.5 Fe and 4.8 ± 0.3 S^{2-} (Supplementary Table 4). A sequence alignment of KgrC and SuiB, a RaS enzyme for which the crystal structure has been solved,[27,28] revealed a SPASM domain in KgrC that may bind two [4Fe-4S] clusters in addition to the active site cluster (Supplementary Fig. 2). Our preparation of KgrC was likely not fully reconstituted, though chemical reconstitution was not necessary to obtain active protein. The third biosynthetic enzyme, KgrD, a predicted arginase homolog, was purified aerobically with supplemental Mn^{2+}.

With all components available, *in vitro* reactions were carried out by incubating KgrA with each enzyme alone, with each combination of two enzymes, or with all three enzymes. All reactions contained SAM, DTT, and reductant (titanium citrate). Following overnight incubation under anerobic conditions, reactions were digested with trypsin or GluC to give peptide fragments small enough to allow for analysis by HPLC-Qtof-MS (Supplementary Tables 5-6). No new products were observed following incubation of KgrA with KgrB, KgrD, or KgrB and KgrD (Supplementary Fig. 3). However, reaction with KgrC alone gave a product 2 Da lighter than substrate (Fig. 2a). While KgrC and KgrB only revealed the -2 Da product (Supplementary Fig. 3), the reaction with KgrC and KgrD yielded product that was 44 Da lighter than the substrate in addition to a small amount of remaining -2 Da product (Fig. 2a). Finally, the reaction with all three biosynthetic enzymes resulted in formation of a product peak that was 30 Da lighter than the

original KgrA substrate, or 14 Da heavier than the product of the KgrCD reaction (Fig. 2a). This species was only observed in the presence of all three biosynthetic enzymes and was assigned as the final reaction product.

KgrC, a Thiomorpholine-forming RaS Enzyme. We first used HR-MS/MS to analyze the GluC-treated products after reaction of KgrA with KgrC, KgrCD, or KgrBCD (Supplementary Tables 7-10). With KgrA alone, nearly all expected b and y-ions of the unmodified peptide were observed. Upon reaction with KgrC, all b ions upstream of Arg41 were unaltered, whereas those downstream were -2 Da relative to untreated KgrA. Likewise, y ions downstream of Arg41 were unaltered whereas those upstream were -2 Da (Fig. 2b). An α-thioether bond with the adjacent Cys residue would be consistent with the HR-MS and the fragmentation pattern observed as these linkages are known to undergo in-source retro-elimination during MS/MS leading to a 2 Da mass loss on the acceptor residue.[29] In the absence of KgrA, KgrC produced 5'-deoxyadenosine (5'-dA), a futile cycling reaction of cofactor SAM that is diagnostic for RaS enzymes. Moreover, in the presence of KgrA, the release of 5'-dA and product occurred with similar kinetics (Supplementary Fig. 4); the reaction was strictly dependent on SAM and reductant (Fig. 2c). We conclude that KgrC is a RaS enzyme that installs the smallest sactionine linkage to date, leading to a novel thiomorpholine modification in the KgrA backbone. The absolute configuration of the newly formed quaternary center at the Arg α-carbon remains to be determined.

KgrD, a RiPP Arginase. Next, we analyzed the product resulting from the reaction of KgrA with KgrCD. All b ions upstream of Arg41 were unaltered, whereas those downstream were now 44 Da lighter than unreacted KgrA (Fig. 2b). The y fragments mirrored this pattern and isolated residue 41 as the target of the KgrD-catalyzed modification. The HR-MS was entirely consistent with loss of the guanidinium group giving rise to an ornithine sidechain at this position. We examined the modification further by purifying KgrD in the absence or presence of Mn^{2+} and incubating it with the product of the KgrAC reaction; the Mn^{2+}-reconstituted enzyme showed the highest activity (Supplementary Fig. 5). Together, these results suggest that KgrD is an Mn^{2+}-dependent enzyme that hydrolyzes the Arg41 guanidinium group, only after thiomorpholine formation, giving rise to an ornithine sidechain.

KgrB, an Fe-S-dependent Methyltransferase. Finally, we analyzed the product of the KgrBCD reaction by HR-MS/MS and noted that the b and y ion fragments point to a 14 Da increase at the newly-generated Orn residue, suggesting KgrB may install a methyl group (Fig 2b). To

determine the exact nature of the modification and provide additional support for the products of KgrC and KgrD, we carried out the KgrABCD reaction on a large scale and conducted detailed 1D/2D NMR analysis after trypsinolysis of the product to a 17mer peptide. An unmodified 17mer was synthesized via solid-phase peptide synthesis as a reference and analyzed by 1D/2D NMR in a similar manner (Supplementary Table 11, Supplementary Fig. 6-7). ^{1}H and TOCSY NMR analysis revealed correlations from the Arg-δH to the α-, β-, and γ-Hs in the substrate (Fig. 3a). In the product, however, the correlation from the Orn-δH to an α-H was missing, and the β-, γ-, and δ-carbons were clearly methylenes, as indicated by HSQC, all consistent with a modification at the Orn-αC (Fig. 3b). In addition, the peaks assigned to the adjacent Cys-αH and βHs shifted from 4.88 and 2.75/3.10 ppm in the substrate to 4.76 and 3.07/3.28 ppm, respectively, in the product. These shifts are expected for an α-thioether, thereby establishing the proposed thiomorpholine installation. The ^{1}H NMR spectrum also revealed a new methyl-singlet peak at 2.59 ppm with an associated 32.7 ppm ^{13}C shift (Supplementary Fig. 6). HMBC correlations from the methyl-protons to the Orn-δC (Fig. 3c, 3d) and a ROESY correlation (Fig. 3e) to the Orn-δH established this feature as the N-methyl group of Orn. These data, together with the HR-MS and HR-MS/MS results above, point to three unusual transformations, consisting of thiomorpholine formation by the RaS enzyme, followed by Mn^{2+}-dependent deguanidination by KgrD, and finally Orn N-methylation by the Fe-S-containing KgrB (Fig 3f).

A New Superfamily of Fe-S Methyltransferases. We were intrigued by the novel Fe-S-dependent *N*-methylation and investigated this reaction further *in vitro* and bioinformatically. The latter showed that KgrB does not significantly match any Pfam in the available protein database. A PSI-BLAST search with the KgrB sequence allowed us to generate an SSN with the 5,000 top hits (Supplementary Fig. 8). Nearly all identified proteins were annotated as a domain of unknown function, uncharacterized protein, or hypothetical protein. Interestingly, 40 of the 5,000 proteins were annotated as Flagellin N-methylase,[30,31] which would indicate a similar activity to KgrB. The Flagellin N-methylase protein, FliB, has been studied through genetic approaches, though not yet biochemically, and was proposed to methylate flagellar Lys residues in *Salmonella typhimurium*.[30,31] While FliB and KgrB share only 11% sequence similarity, they appear catalyze similar reactions; a sequence alignment of the two proteins shows a conserved CxxxCC motif along with several other conserved Cys residues (Supplementary Fig. 9). Additionally, a LogoPlot of the top 5,000 PSI-BLAST hits shows that this CxxxCC motif is conserved among the entire family

(Supplementary Fig. 10). These analyses show that enzymes in the Fe-S methyltransferase family are wide-spread without a single biochemically characterized member.

To characterize KgrB further, we first prepared sufficient amounts of the KgrB substrate using a heterologous co-expression system in which a maltose binding protein-tagged KgrA was co-expressed with KgrC and KgrD on a pRSFDuet vector in *E. coli*. Upon purification, we confirmed presence of the Orn-thiomorpholine modification (Supplementary Table 12). After reaction with KgrB, we observed time- and enzyme-dependent formation of the N-methyl product (Supplementary Fig. 11), which required SAM, substrate, and KgrB, but not reductant (Fig. 4a), suggesting that SAM served as the methyl donor. To verify, we repeated the reaction with S-(methyl-*d3*)-S-adenosylmethionine (*d3*-SAM) and observed a product that was now +3 Da relative to the control reaction with protonated SAM (Fig. 4b, 4c). HR-MS/MS analysis confirmed that the deuterated methyl group was located on the Orn sidechain (Supplementary Table 13). The other product, S-adenosylhomocysteine (SAH), was difficult to identify directly because of significant levels of SAH in the commercial SAM preparations and continuous degradation of SAM to SAH, a previously reported side-reaction,[32,33] even after purification of SAM. We also monitored 5'-dA formation and found that KgrB could generate small amounts in the presence of reductant. However, 5'-dA formation was minimal in the absence of reductant and did not correlate with product formation (Supplementary Fig. 12). Together, our results provide the first biochemical characterization of this superfamily of Fe-S-dependent methyltransferases.

Discovery of Enteropeptins from E. cecorum. We next used insights into the reactions of the biosynthetic enzymes to search for the mature product of the *kgr* cluster in *E. cecorum* ATCC 43198. Based on general RiPP biosynthetic logic, we compiled a list of *m/z* values of potential mature peptides containing the modifications elucidated above and trimmed either *N*-terminal to Arg41 and/or *C*-terminal to Pro43. *E. cecorum* ATCC 43198 was then cultured to stationary phase, the supernatant cleared by solid phase extraction, and subsequently analyzed by HPLC-Qtof-MS. Any species that matched the *m/z* in the compiled list was further characterized by HR-MS/MS. Three candidates emerged, the most abundant comprising an 8mer peptide containing the N-methylOrn-thiomorpholine modification. MS/MS analysis showed b and y ions consistent the with the sequence of the peptide and the fragmentation pattern observed in the enzymatic reactions (Supplementary Table 14). In addition, two minor variants, 7mer and 9mer products, were also observed and confirmed by HR-MS/MS to carry the N-methylOrn-thiomorpholine alteration

(Supplementary Tables 15-16). These products could result from the predicted transporter, KgrE, cleaving C-terminally to both Ser37 and Ser45 to give the 8mer product but occasionally cleaving N-terminally yielding the 7mer or 9mer products. Alternatively, other proteases may be involved.

To provide further support that these peptides are the mature *kgr* products, we prepared a synthetic standard via an *in vitro* reaction with the purified biosynthetic enzymes and a modified KgrA substrate. Site-directed mutagenesis was used to insert a GluC-site and an AspN-site upstream of Met38 and downstream of Ser45, respectively. The di-substituted KgrA was purified and used as a substrate for an *in vitro* reaction with KgrC, KgrD, and KgrB. The resulting product was treated with GluC/AspN to deliver the modified 8mer peptide. This standard gave the expected HR-MS and HR-MS/MS fragments (Supplementary Table 17), indicating it contained the modifications outlined above. It was then compared to the authentic 8mer isolated from *E. cecorum*. The two peptides showed identical chromatographic properties and co-eluted when injected onto the HPLC-MS in a 1:1 ratio (Fig. 5a). We conclude that the mature product of the *kgr* gene cluster is this 8mer RiPP which we have named enteropeptin A (Fig. 5b). It is synthesized by a sequence of four modifications, thiomorpholine formation by KgrC, deguanidination by KgrD, methylation of the resulting Orn group by KgrB, and finally removal of the leader and follower sequences by KgrE and perhaps another protease (Fig. 5c). The 7mer and 9mer products, termed enteropeptin B and C, form two less abundant products of the *kgr* operon.

Narrow-spectrum Bacteriostatic Activity. As a starting point to examine enteropeptin A's activity, we first determined its timing of production. The RaS-RiPPs in our network are controlled by an *shp-rgg* QS operon and their products accumulate starting in mid-exponential phase.[34,35] Similarly, the *kgr* cluster in *E. cecorum* is controlled by a LytTR-type regulator,[26] and enteropeptin A synthesis as a function of growth, as determined by optical density at 600 nm (OD_{600}), revealed production in mid-exponential phase that persisted into stationary phase, reaching a maximal concentration of 0.7 μM (Fig. 6a).

With pure material at hand and clues regarding production titers, we tested the effect of 0.1–3 μM enteropeptin A on a number of microbiome strains, including *Staphylococcus aureus, Pseudomonas aeruginosa, E. coli, Enterococcus faecalis, Streptococcus thermophilus,* and *Enterococcus cecorum* (Supplementary Table 18). Enteropeptin A only inhibited the growth of *E. cecorum* and did not affect the other strains. A growth curve of *E. cecorum* in the presence of various concentrations of enteropeptin A, or the linear 8mer as control, showed a concentration-

dependent growth cessation only with mature product; the linear 8mer had no effect (Fig. 6b). The observed growth inhibition, however, appeared bacteriostatic as the OD_{600} eventually recovered. Whether enteropeptin A is fratricidal or plays a role in regulating growth by different means remains to be determined.

Discussion

Enteropeptins add to the growing list of sactipeptides but are distinct from those discovered thus far, as they contain the smallest sactionine linkage yet in the form of a thiomorpholine heterocycle. The majority of mature sactipeptides belong to Type 1 with multiple nested thioether macrocycles and at least two residues between the acceptor and donor residues.[36] Type 2 sactipeptides, streptosactin and the product from the QMP cluster, carry an unnested bicycle topology.[17] Enteropeptins now add another distinct chemotype, for which we propose the Type 3 sactipeptide designation.

A further distinguishing feature from sactipeptides so far is the additional modifications in enteropeptins. Thuricin α and β,[37] thurincin H,[38] huazacin/thuricin Z,[39,40] and ruminococcin C[41,42] contain only thioether linkages while SKF and subtilosin carry head-to-tail amide cyclizations,[43-47] with the former additionally harboring a disulfide linkage. The presence of ornithine is well-documented in nonribosomal peptides; N-methylornithine, however, is a novel unit for RiPP natural products. The incorporation of ornithine was very recently reported in the heterologous landornamide product.[48,49] The use of an arginase homolog to generate ornithine in RiPPs and to modify it further represents a backdoor route for the incorporation and diversification of unnatural amino acids into ribosomally-generated products.[50]

Perhaps the most surprising discovery from this study is KgrB, the first characterized member of an enzyme superfamily of Fe-S-dependent methyltransferases. Only one other example of an Fe-S methyltransferase has previously been described; RumA catalyzes the methylation of U1939 of 23S ribosomal RNA to yield 5-methyluridine or ribothymidine.[51] A crystal structure of the enzyme shows that the Fe-S cluster is located in the RNA-binding domain of the protein and is ligated by four cysteines with a $CX_5CX_2CX_nC$ motif.[52] The Fe-S cluster was proposed to facilitate protein folding or RNA binding rather than a catalytic role. Though KgrB and RumA contain Fe-S clusters and catalyze methylation reactions, they are unrelated and belong to distinct structural families and enzyme phylogenies. The two proteins share only 8% sequence identity and

RumA does not contain the characteristic CxxxCC motif found in KgrB and other superfamily members (Supplementary Fig. 13). While it is tempting to speculate catalytic roles for the KgrB Fe-S cluster, such as a Lewis acid catalysis to activate the Orn amnio group for nucleophilic attack, additional studies are required to elucidate the mechanism of KgrB and provide insights into the chemistry underlying this unusual methylation strategy.

Enteropeptins builds an emerging theme of RaS-RiPPs in firmicutes that show species-specific growth-inhibitory activity against the host. Aside from the streptococcal RiPPs, streptosactin, and tryglysin, the *B. subtilis* product SKF, subtilosin, and YydF also show varying levels of inhibitory activity against the host.[53,54] Whether these molecules act as true fratricidal agents that cause cell lysis or merely inhibit growth through other mechanisms remains to be delineated.[55,56] As the first natural product identified from *E. cecorum*, enteropeptins point the way to a new source of microbiome natural products. Host-associated firmicutes have not been thought of as prolific producers of secondary metabolites but the discovery of new RiPPs show that these bacteria, and others associated with mammalian microbiomes, harbor a vast and poorly explored biosynthetic capacity that is now ripe to be mined.

Acknowledgments

We thank the Edward C. Taylor-Eli Lilly Fellowship in Chemistry (to K.A.C.) and the National Science Foundation (NSF CAREER Award 1847932 to M.R.S.) for support of this work.

References

1. Fischbach, M. A. & Walsh, C. T. Assembly-Line Enzymology for Polyketide and Nonribosomal Peptide Antibiotics: Logic, Machinery, and Mechanisms. *Chem. Rev.* **106,** 3468-3496 (2006).
2. Montalbán-López, M. et al. New developments in RiPP discovery, enzymology and engineering. *Nat. Prod. Rep.* **38,** 130-239 (2021).
3. The Human Microbiome Project Consortium. Structure, function and diversity of the healthy human microbiome. *Nature* **486,** 207–214 (2012).
4. Donia, M. S. et al. A systematic analysis of biosynthetic gene clusters in the human microbiome reveals a common family of antibiotics. *Cell* **158,** 1402-1414 (2014).
5. Bushin, L. B., Clark, K. A., Pelczer, I. & Seyedsayamdost, M. R. Charting an Unexplored Streptococcal Biosynthetic Landscape Reveals a Unique Peptide Cyclization Motif. *J. Am. Chem. Soc.* **140**, 17674-17684 (2018).
6. Russell, A. H. & Truman, A. W. Genome mining strategies for ribosomally synthesised and post-translationally modified peptides. *Comput. Struct. Biotechnol. J.* **18,** 1838-1851 (2020).
7. Hetrick, K. J. & van der Donk, W. A. Ribosomally synthesized and post-translationally modified peptide natural product discovery in the genomic era. *Curr. Opin. Chem. Biol.* **38,** 36-44 (2017).
8. Kloosterman, A. M., Medema, M. H., & van Wezel, G. P. Omics-based strategies to discover novel classes of RiPP natural products. *Curr. Opin. Biotechnol.* **69,** 60-67 (2021).

9. Tietz, J. I., & Mitchell, D. A. Using Genomics for Natural Product Structure Elucidation. *Curr. Top Med. Chem.* **16,** 1645-94 (2016).
10. Schramma, K. R., Bushin, L. B. & Seyedsayamdost, M. R. Structure and biosynthesis of a macrocyclic peptide containing an unprecedented lysine-to-tryptophan crosslink. *Nature Chem* **7,** 431–437 (2015).
11. Ibrahim, M. et al. Control of the transcription of a short gene encoding a cyclic peptide in *Streptococcus thermophilus*: a new quorum-sensing system? *J. Bacteriol*. **189**, 8844–8854 (2007).
12. Broderick, J. B., Duffus, B. R., Duschene, K. S. & Shepard, E. M. Radical S-adenosylmethionine enzymes. *Chem. Rev*. **114**, 4229–4317 (2014).
13. Landgraf, B. J., McCarthy, E. L. & Booker, S. J. Radical S-Adenosylmethionine Enzymes in Human Health and Disease. *Annu. Rev. Biochem.* **85,** 485-514 (2016).
14. Bassler, B. L. & Losick, R. Bacterially speaking. *Cell* **125,** 237-46 (2006).
15. Whiteley, M., Diggle, P. S. & Greenberg, E. P. Progress in and promise of bacterial quorum sensing research. *Nature* **551,** 313-320 (2017).
16. Rued, B. E. et al. Quorum Sensing in *Streptococcus mutans* Regulates Production of Tryglysin, a Novel RaS-RiPP Antimicrobial Compound. *mBio* **12,** e02688-20 (2021).
17. Bushin, L. B., Covington, B. C., Rued, B. E., Federle, M. J. & Seyedsayamdost, M. R. Discovery and Biosynthesis of Streptosactin, a Sactipeptide with an Alternative Topology Encoded by Commensal Bacteria in the Human Microbiome. *J. Am. Chem. Soc.* **142,** 16265-16275 (2020).
18. Caruso, A. & Seyedsayamdost, M. R. Radical SAM Enzyme QmpB Installs Two 9-Membered Ring Sactionine Macrocycles during Biogenesis of a Ribosomal Peptide Natural Product. *J. Org. Chem.* **86,** 11284-11289 (2021).
19. Clark, K. A., Bushin, L. B. & Seyedsayamdost, M. R. Aliphatic Ether Bond Formation Expands the Scope of Radical SAM Enzymes in Natural Product Biosynthesis. *J. Am. Chem. Soc.* **141,** 10610-10615 (2019).
20. Caruso, A., Bushin, L. B., Clark, K. A., Martinie, R. J. & Seyedsayamdost, M. R. Radical Approach to Enzymatic β-Thioether Bond Formation. *J. Am. Chem. Soc.* **141,** 990-997 (2019).
21. Caruso, A., Martinie, R. J., Bushin, L. B. & Seyedsayamdost, M. R. Macrocyclization via an Arginine-Tyrosine Crosslink Broadens the Reaction Scope of Radical S-Adenosylmethionine Enzymes. *J. Am. Chem. Soc.* **141,** 16610-16614 (2019).
22. Burkhart, B. J., Hudson, G. A., Dunbar, K. L. & Mitchell, D. A. A prevalent peptide-binding domain guides ribosomal natural product biosynthesis. *Nat. Chem. Biol.* **11,** 564-570 (2015).
23. Kanyo, Z. F., Scolnick, L. R., Ash, D. E. & Christianson, D. W. Structure of a unique binuclear manganese cluster in arginase. *Nature* **383,** 554–557 (1996).
24. Ash D.E., Cox J. D. & Christianson D.W. Arginase: a binuclear manganese metalloenzyme. *Met. Ions Biol. Syst.* **37,** 407-28 (2000).
25. Jung A., Chen L. R., Suyemoto M. M., Barnes H. J. & Borst L. B. A Review of Enterococcus cecorum Infection in Poultry. *Avian Dis.* **62,** 261-271 (2018).
26. Do, T., Page, J. E. & Walker, S. Uncovering the activities, biological roles, and regulation of bacterial cell wall hydrolases and tailoring enzymes. *J. Biol. Chem.* **295,** 3347-3361 (2020).
27. Davis, K. M. et al. Structures of the peptide-modifying radical SAM enzyme SuiB elucidate the basis of substrate recognition. *Proc. Natl. Acad. Sci. U. S. A.* **114,** 10420-10425 (2017).
28. Schramma, K. R. & Seyedsayamdost, M. R. Lysine-Tryptophan-Crosslinked Peptides Produced by Radical SAM Enzymes in Pathogenic Streptococci. *ACS Chem. Biol.* **12,** 922-927 (2017).
29. Himes, P. M. Allen, S. E., Hwang, S. & Bowers, A. A. Production of Sactipeptides in Escherichia coli: Probing the Substrate Promiscuity of Subtilosin A Biosynthesis. *ACS Chem. Biol.* **11,** 1737-1744 (2016).
30. Tronick S. R. & Martinez R. J. Methylation of the flagellin of *Salmonella typhimurium*. *J. Bacteriol.* **105,** 211- 219 (1971).
31. Stocker, B. A. D., McDonough, M. W. & Ambler, R. P. A gene determining presence or absence of e-N-methyllysine in *Salmonella* flagellar protein. *Nature* **189,** 556-558 (1961).
32. Lankau, T., Kuo, T. N & Yu, C. H. Computational Study of the Degradation of S-Adenosyl Methionine in Water. *J. Phys. Chem. A.* **121,** 505-514 (2017).
33. Salyan, M. E. K. et al. A general liquid chromatography/mass spectroscopy-based assay for detection and quantitation of methyltransferase activity. *Anal. Biochem.* **349,** 112-117 (2006).
34. Fleuchot, B. et al. Rgg proteins associated with internalized small hydrophobic peptides: a new quorum-sensing mechanism in streptococci. *Mol. Microbiol*. **80**, 1102–1119 (2011).

35. Chang, J. C., LaSarre, B.,Jimenez, J. C., Aggarwal, C. & Federle, M. J. Two Group A Streptococcal Peptide Pheromones Act through Opposing Rgg Regulators to Control Biofilm Development. *PLoS Pathog.* 7, e1002190 (2011).
36. Flühe, L. & Marahiel, M. A. Radical S-adenosylmethionine enzyme catalyzed thioether bond formation in sactipeptide biosynthesis. *Curr. Opin. Chem. Biol*. **17,** 605-12 (2013).
37. Rea, M. C. et al. Thuricin CD, a Posttranslationally Modified Bacteriocin with a Narrow Spectrum of Activity against *Clostridium difficile*. *Proc. Natl. Acad. Sci. U. S. A.* **107,** 9352- 9357 (2010).
38. Lee, H., Churey, J. J. & Worobo, R. W. Biosynthesis and transcriptional analysis of thurincin H, a tandem repeated bacteriocin genetic locus, produced by *Bacillus thuringiensis* SF361. *FEMS Microbiol. Lett.* **299,** 205-213 (2009).
39. Hudson, G. A. et al. Bioinformatic Mapping of Radical S-Adenosylmethionine-Dependent Ribosomally Synthesized and Post-Translationally Modified Peptides Identifies New Cα, Cβ, and Cγ-Linked Thioether-Containing Peptides. *J. Am. Chem. Soc.* **141,** 8228- 8238 (2019).
40. Mo, T. et al. Thuricin Z: A Narrow-Spectrum Sactibiotic that Targets the Cell Membrane. *Agnew. Chem. Int. Ed.* **58,** 18793- 18797 (2019).
41. Chiumento, S. et al. Ruminococcin C, a promising antibiotic produced by a human gut symbiont. *Sci. Adv.* **5,** eaaw9969 (2019).
42. Balty, C. et al. Ruminococcin C, an anti-clostridial sactipeptide produced by a prominent member of the human microbiota *Ruminococcus gnavus. J. Biol. Chem.* **294,** 14512-14525 (2019).
43. Kawulka, K. E. et al. Structure of subtilosin A, an antimicrobial peptide from *Bacillus subtilis* with unusual posttranslational modifications linking cysteine sulfurs to alpha-carbons of phenylalanine and threonine. *J. Am. Chem. Soc.* ***125*****,** 4726– 4727 (2003).
44. Kawulka, K. E. et al. Structure of Subtilosin A, a Cyclic Antimicrobial Peptide from Bacillus Subtilis with Unusual Sulfur to α-Carbon Cross-Links: Formation and Reduction of α-Thio-α-Amino Acid Derivatives. *Biochemistry **43*****,** 3385– 3395 (2004).
45. Flühe, L. et al. Two [4Fe-4S] Clusters Containing Radical SAM Enzyme SkfB Catalyze Thioether Bond Formation during the Maturation of the Sporulation Killing Factor. *J. Am. Chem. Soc.* **135,** 959- 962 (2013).
46. Lui, W.-T., et al. Imaging mass spectrometry of intraspecies metabolic exchange revealed the cannibalistic factors of Bacillus subtilis. *Proc. Natl. Acad. Sci. U. S. A.* **107,** 16286-16290 (2010).
47. Flühe, L. et al. The radical SAM enzyme AlbA catalyzes thioether bond formation in subtilosin A. *Nat. Chem. Biol.* **8,** 350- 357 (2012).
48. Bösch, N. M. et al. Landornamides: Antiviral Ornithine-Containing Ribosomal Peptides Discovered through Genome Mining. *Angew. Chem. Int. Ed.* **59**, 11763-11768 (2020).
49. Mordhorst S., Morinaka B. I., Vagstad A. L. & Piel J. Posttranslationally Acting Arginases Provide a Ribosomal Route to Non-proteinogenic Ornithine Residues in Diverse Peptide Sequences. *Angew. Chem. Int. Ed.* **59,** 21442-21447 (2020).
50. Walsh, C. T. Blurring the lines between ribosomal and nonribosomal peptide scaffolds. *ACS Chem. Biol.* **9,** 1653- 1661 (2014).
51. Agarwalla, S., Kealey, J. T., Santi, D. V. & Stroud, R. M. Characterization of the 23 S Ribosomal RNA m^5U1939 Methyltransferase from *Escherichia coli. J. Biol. Chem.* **277,** 8835-8840 (2002).
52. Lee, T. T., Agarwalla, S. & Stroud, R. M. Crystal structure of RumA, an iron-sulfur cluster containing E. coli ribosomal RNA 5-methyluridine methyltransferase. *Structure* **12,** 397-407 (2004).
53. Benjdia, A., Guillot, A., Ruffié, P. *et al.* Post-translational modification of ribosomally synthesized peptides by a radical SAM epimerase in *Bacillus subtilis*. *Nature Chem* **9,** 698–707 (2017).
54. Chen, Y., Wang, J., Li, G., Yang, Y. & Ding, W. Current advancements in sactipeptide natural products. *Front. Chem.* **9,** 595991 (2021).
55. Claverys, J.-P., Martin, B. & Håvarstein, L. S. Competence-induced Fratricide in Streptococci. *Mol. Microbiol.* **64,** 1423- 1433 (2007).
56. Claverys, J.-P. & Håvarstein, L. S. Cannibalism and fratricide: mechanisms and raisons d'être. *Nat. Rev. Microbiol.* **5,** 219–229 (2007).

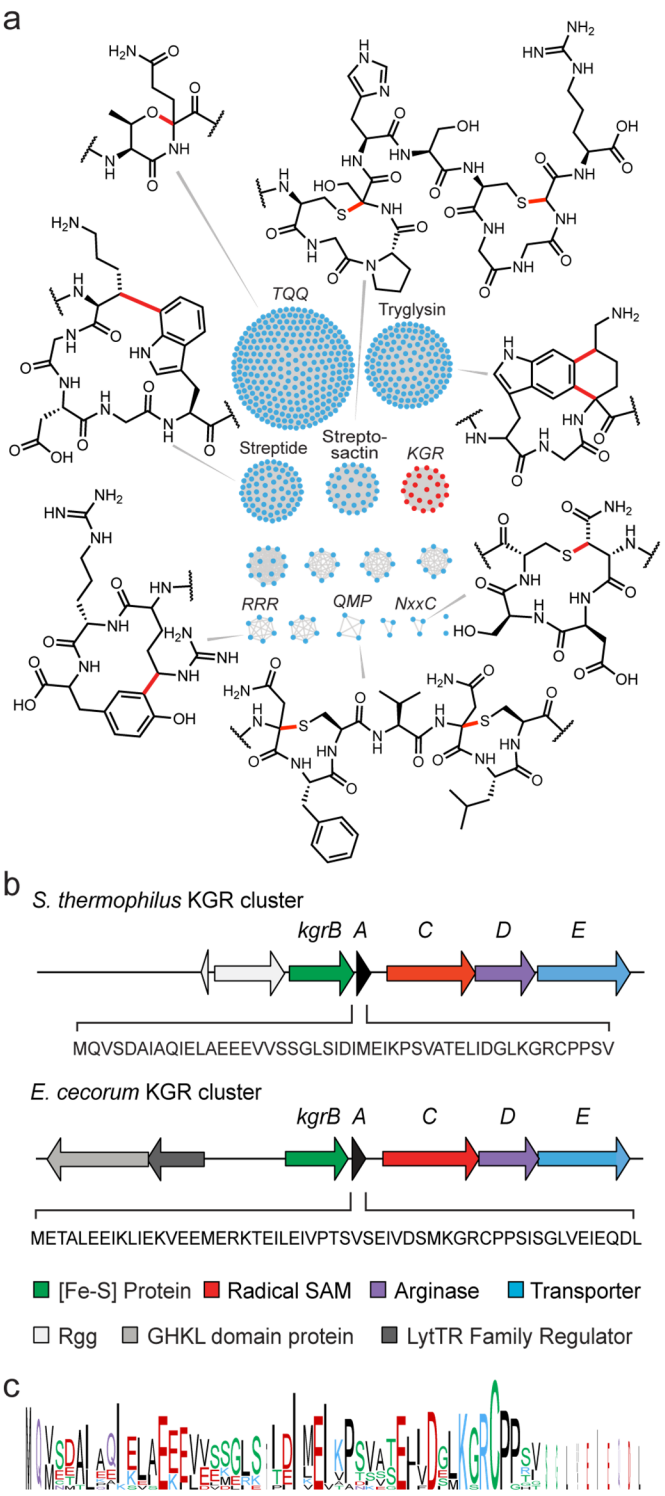

Figure 1. Streptococcal RaS-RiPPs and the *kgr* gene cluster. (a) SSN of RaS-RiPP BGCs regulated by QS. Each node represents a unique BGC, and the lines indicate sequence similarity of the precursor peptide. Subfamilies are named based on conserved motifs in the precursor. Known products of RaS enzymes in each subfamily are shown with the newly installed bond in red. For the streptide, streptosactin, and tryglysin subfamilites, the mature product is known. (b) The *kgr* BGC from *S. thermophilus* and *E. cecorum*. Sequences of precursor peptides are shown. (c) Sequence logo plot for all known KgrA peptides. The KGRCPP motif is conserved.

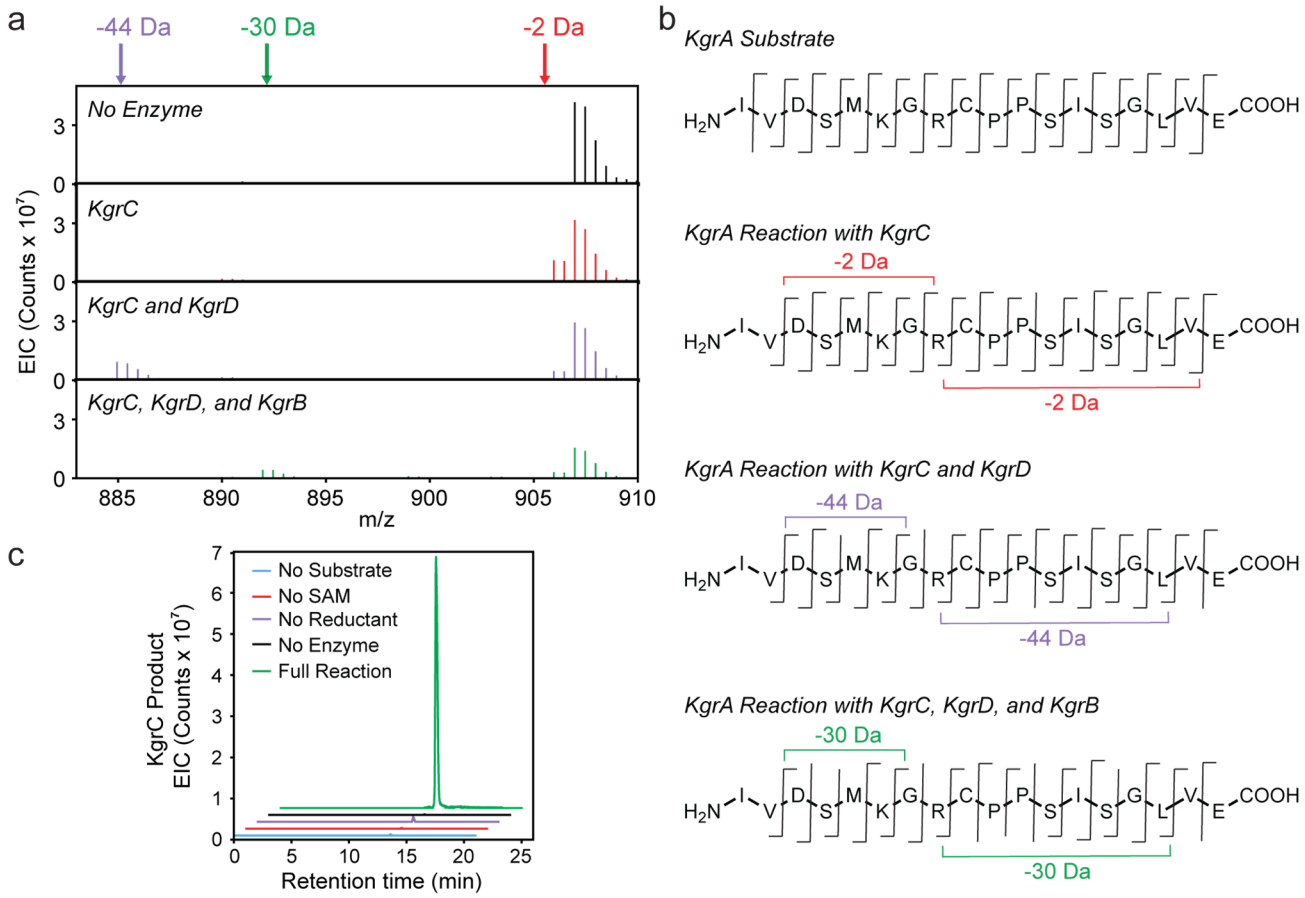

Figure 2. Reactions of KgrBCD characterized by HR-MS and HR-MS/MS. (a) MS profiles of the reactions of KgrA with KgrC, KgrCD, and KgrBCD. Products for each reaction are marked and color-coded. (b) HR-MS/MS profiles of the reaction of KgrA with KgrC, KgrCD, and KgrBCD. Observed fragments and the mass difference relative to the unreacted KgrA peptide are marked. (c) HPLC-MS analysis of the reaction of KgrC with KgrA. Product formation is only observed in the full reaction.

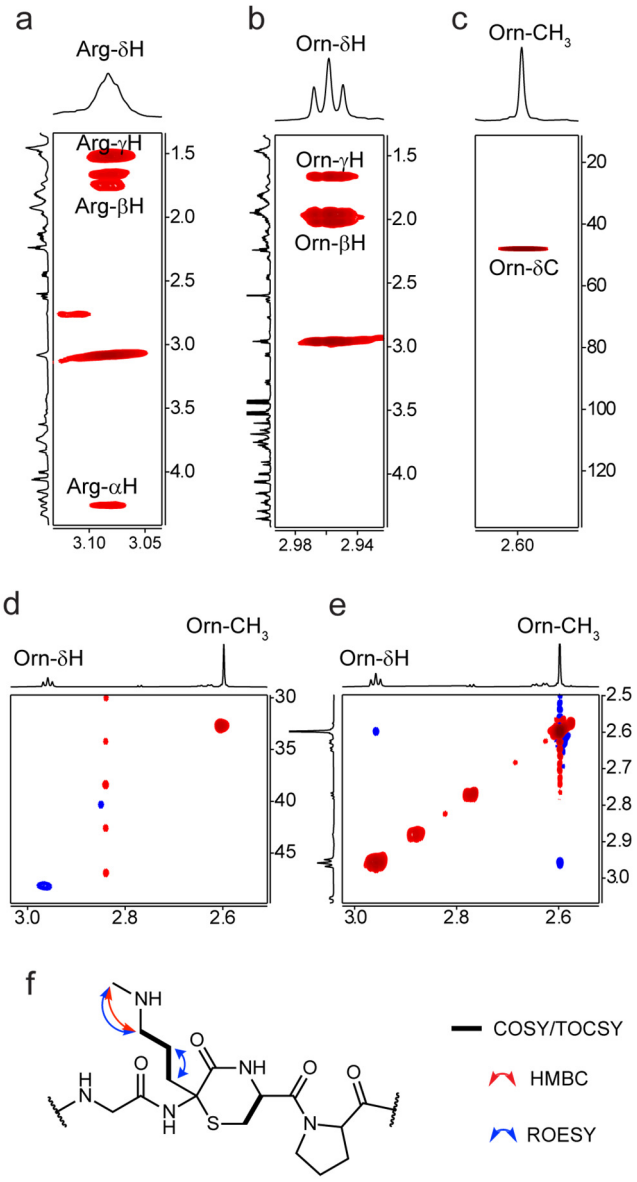

Figure 3. NMR spectral analysis of the product of the reaction of KgrA with KgrBCD. (a, b) TOCSY slice of the Arg41-γH (precursor peptide numbering) in unreacted KgrA (a) compared to the corresponding Orn-γH in product (b). An α-H is not observed in the product. (c) HMBC slice of the N-methyl group of Orn shows a crosspeak to the Orn-γC. (d) HSQC spectrum highlighting the Orn N-methyl-H/C and Orn-γH/γC correlations. (e) ROESY spectrum showing crosspeaks between the Orn-γH and N-methyl group. (f) Structure of the product of the KgrABCD reaction focusing on the modified region. Relevant NMR correlations are shown. The absolute configuration at the Orn α-C remains to be determined.

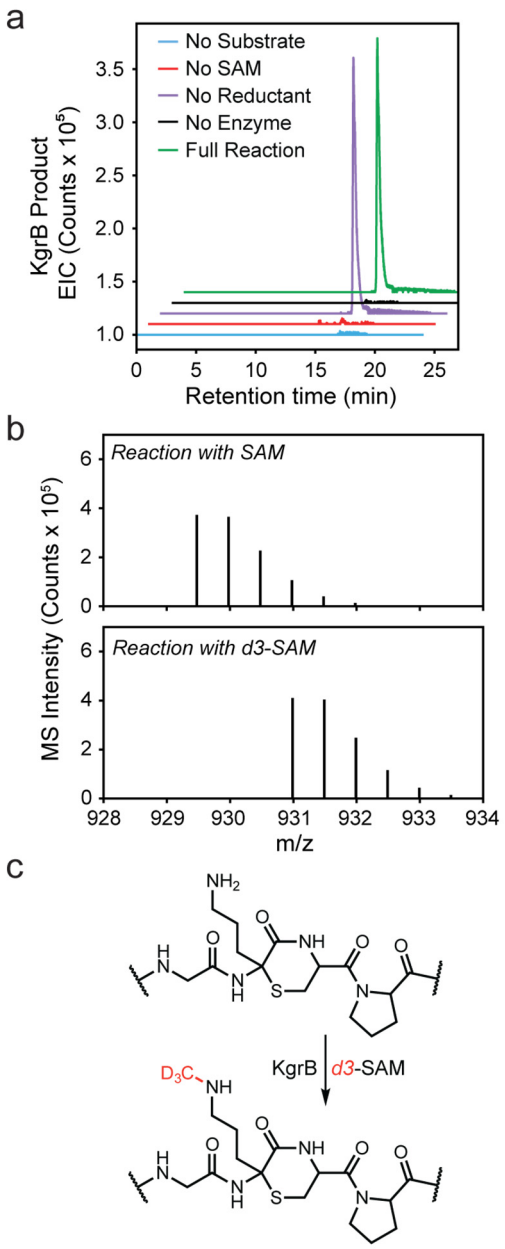

Figure 4. Orn N-methylation catalyzed by KgrB. (a) HPLC-MS analysis of the reaction of KgrB with the product of KgrACD. Reductant is not required but SAM is. (b) Reaction with *d3*-SAM gives a corresponding +3 Da increase relative to the product with protonated SAM. (c) Reaction carried out by KgrB with *d3*-SAM.

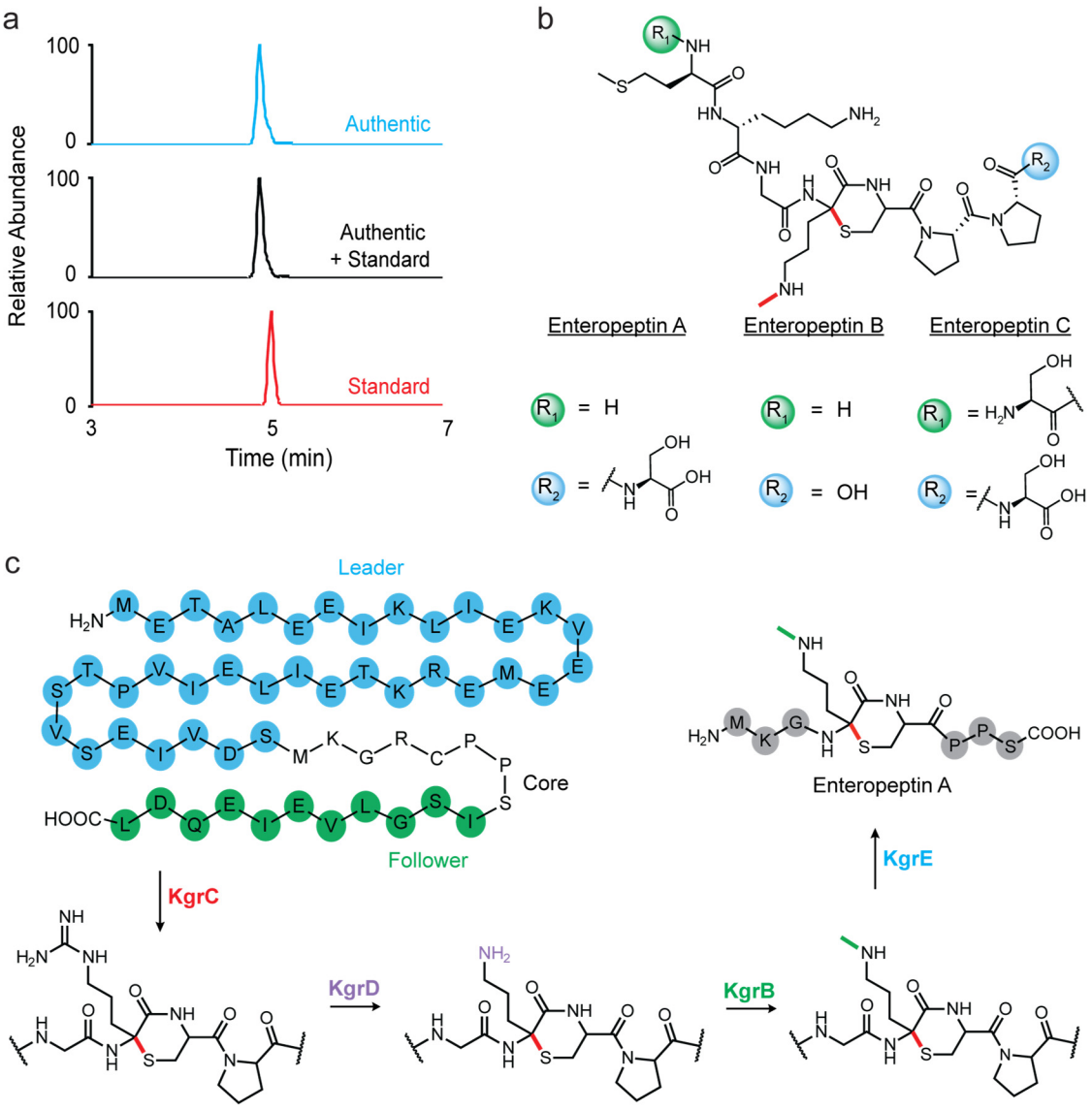

Figure 5. Discovery of enteropeptins, the mature product of the *kgr* cluster, from *E. cecorum*. (a) HPLC-Qtof-MS analysis of authentic and synthetic enteropeptin A. Shown are extracted ion chromatograms for authentic enteropeptin from *E. cecorum* (blue, top), heterologously produced enteropeptin (red, bottom), and a 1:1 coinjection of these two samples (black, middle), which coelute. (b) Structures of enteropeptin A, the major product of the *kgr* cluster, and of minor products enteropeptin B and C. (c) Biosynthetic pathway for enteropeptins. Leader and follower sequences are indicated with blue and green spheres, respectively. Unmodified amino acids in the final product are shown in gray spheres.

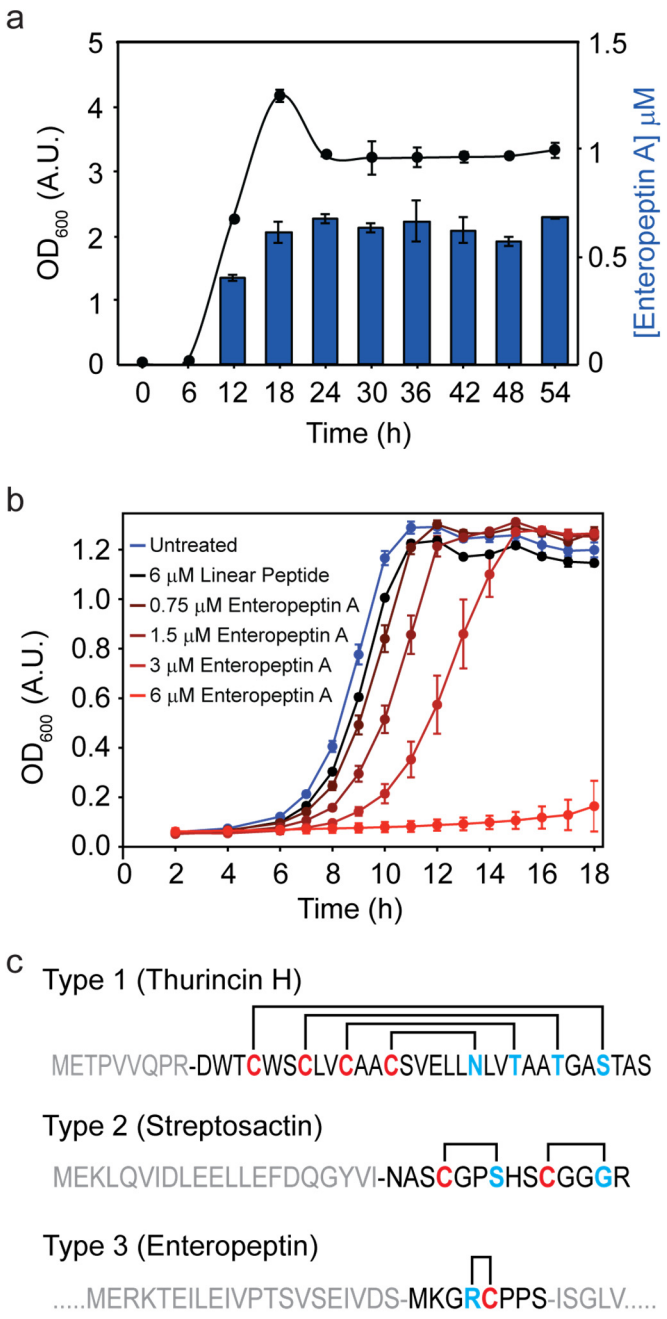

Figure 6. Enteropeptin activity and compound class. (a) Enteropeptin is synthesized starting in exponential phase and reaches a maximal concentration of ~0.7 µM in stationary phase. (b) Enteropeptin bacteriostatically inhibits *E. cecorum* growth. Shown are growth curves of *E. cecorum* in the presence of 0.75–6 µM of enteropeptin A. No effect is seen with 6 µM of unmodified, linear core peptide. (c) Comparison of the topology of known Type 1 and Type 2 sactipeptides, represented by thurincin H and streptosactin respectively, with enteropeptin as a new Type 3 sactipeptide. Leader/follower sequences are shown in gray. Note, only partial leader/follower sequences are shown for enteropeptin.